Calcif Tissue Int (2008) 82:316–326
DOI 10.1007/s00223-008-9115-8

Ovariectomy Sensitizes Rat Cortical Bone to Whole-Body Vibration

Alessandro Rubinacci · Massimo Marenzana · Francesco Cavani · Federica Colasante · Isabella Villa · Johannes Willnecker · Gian Luigi Moro · Luigi Paolo Spreafico · Marzia Ferretti · Francesca Guidobono · Gastone Marotti

Received: 26 June 2007 / Accepted: 4 February 2008 / Published online: 1 April 2008

Abstract This study was designed to determine the modulatory effect of estrogen on mechanical stimulation in bone. Trabecular and cortical bone compartments of ovariectomized rats exposed to whole-body vibration of different amplitudes were evaluated by peripheral quantitative computed tomographic (pQCT) analysis and histomorphometry and compared to controls not exposed to vibration. Rats underwent whole-body vibration (20 minutes/day, 5 days/week) on a vibration platform for 2 months. The control rats were placed on the platform without vibration for the same time. We divided rats into six groups: a sham control (SHAM); a sham vibrated (SHAM-V) at 30 Hz, 0.6 g; a SHAM-V at 30 Hz, 3g; an ovariectomized control (OVX); an ovariectomized vibrated (OVX-V) at 30 Hz, 0.6 g; and an OVX-V at 30 Hz, 3g. In vivo, pQCT analyses of the tibiae were performed at the start of the experiment and after 4 and 8 weeks. After 8 weeks the tibiae were excised for histomorphometric and for in vitro pQCT analyses. In the SHAM-V group, vibration had no effect upon the different bone parameters. In the OVX-V group, vibration induced a significant increase compared to the OVX group of the cortical and medullary areas ($P < 0.01$) and of the periosteal ($P < 0.01$) and endosteal ($P < 0.05$) perimeters at the 3 g vibration. The strain strength index increased in the OVX-V group significantly ($P < 0.01$) at the higher vibration. The results showed that low-amplitude, high-frequency whole-body vibration is anabolic to bone in OVX animals. The osteogenic potential is limited to the modeling of the bone cortex and depends on the amplitude of the vibration.

Keywords Bone density technology · pQCT · Mechanical loading · Exercise · Mechanotransduction

A. Rubinacci (✉) · M. Marenzana · F. Colasante · I. Villa · G. L. Moro · L. P. Spreafico
Bone Metabolic Unit, Scientific Institute San Raffaele, Via Olgettina 60, Milan 20132, Italy
e-mail: a.rubinacci@hsr.it

F. Cavani · M. Ferretti · G. Marotti
Department of Anatomy and Histology, University of Modena and Reggio Emilia, Modena, Italy

J. Willnecker
Stratec Medizintechnik, Pforzheim, Germany

F. Guidobono
Department of Pharmacology, Chemotherapy, and Medical Toxicology, University of Milan, Milan, Italy

The mechanical signal that modulates bone metabolism includes high-magnitude strains, at frequencies ranging 0.5–2 Hz, and strains of low magnitude at high frequencies reaching 30 Hz. Such strains repeatedly impact bone during various activities, such as standing and muscle contraction. The relevance of these omnipresent, low-level signals was originally characterized by Rubin and coworkers [1]. They demonstrated that low-amplitude mechanical signals, applied by use of a "vibration platform," are associated with modulation of bone mass and morphology by acting on both phases of bone (re)modeling, i.e., resorption and formation [1–3]. Such results confirmed the pioneering observation that chronic vibration tends to increase bone stiffness and microhardness [4]. Recent studies have further characterized the impact of low-amplitude, high-frequency vibration on bone. It can stimulate new trabecular bone formation in sheep [5], expression of osteoblastic genes associated with bone formation and remodeling in mice [6] and in cultured osteoblasts [7], callus formation in a rabbit osteotomy model [8], and new cortical bone

formation in the mouse ulna [9]. The vibratory stimulus can also prevent bone loss and reductions in bone strength in ovariectomized rats [10, 11]. Taken together these data suggest that total-body vibration might differentially affect bone cell activities, thus leading to enhanced bone mass or reduced bone loss associated with estrogen deficiency. However, it remains to be determined whether estrogens modulate the sensitivity of different bone surfaces to a low-amplitude, high-frequency strain. The sensitivity of bone to the mechanical environment is predicted by the mechanostat theory [12], which introduced the concept that a minimum effective strain (MES) must be exceeded in order to stimulate an adaptive response to mechanical overload [13]. Thinking about how a mechanostat system functions in bone physiology led to the hypothesis that nonendocrine factors may influence, in one way or another, the mechanical impact in time and space by modulating MES set-points in a predictable manner. Thus, the anabolic effects of mechanical load under estrogen replacement therapy and the nonresponse of bone to the increased strain under estrogen deficiency were interpreted as a MES down- or upregulation, respectively [14]. However, these targeted shifts of the mechanostat are only able to explain (re)modeling changes at the bone marrow interface (trabecular and endocortical surfaces) where estrogens and strains share a common signaling pathway via estrogen receptor α (ERα) [15, 16]. It has been shown that stimulation by both strain and estrogen results in activation of the extracellular signal–regulated kinase (ERK) pathway, phosphorylation of ERα, and upregulation of the estrogen-responsive element [17, 18]. Moreover, mice lacking functional ERα produce less new cortical bone in response to the same mechanical stimuli as do their ER$\alpha^{+/+}$ littermates [19]. It follows that at least one strain-related cascade responsible for adaptive control of bone architecture is mediated through ERα, activated by estrogen [20]. However, the mechanostat model does not predict the observed changes at the periosteal surface, where estrogens and exercise have opposite effects: exercise enhances periosteal bone formation, while estrogen inhibits it [21]. It is therefore conceivable that estrogens might down- or upregulate the MES set-point, depending upon which bone surface is considered. In humans as well as in rats, estrogen deficiency is accompanied by increased bone size at the appendicular skeleton, which might offset the loss in trabecular bone mass [22–24]. On the other hand, it has also been reported that treatment with estrogens increased bone size in a young man suffering from aromatase deficiency [25]. Based on studies of mice carrying a null mutation of ERβ, signaling through ERβ appears to be the targeted upregulator of the MES set-point that affects the mechanical sensitivity of the periosteum, thus balancing ERα signaling at the bone marrow interface [26]. This evidence led to the conviction that the involvement of sex steroids in mechanical adaptation, particularly periosteal expansion, is more complex than originally believed. Estrogens may regulate the rate of bone remodeling, but bone balance at the surfaces is probably modulated by the prevailing mechanical environment [27].

Taken together these data suggest that mechanical loading can enhance bone (re)modeling at the bone surfaces and might differentially affect bone cell activities, thus leading to enhanced bone mass or reduced bone loss, depending upon estrogen status. This study was therefore designed to test the hypotheses that estrogens modulate the sensitivity of the different bone surfaces to low-amplitude, high-frequency strains and that estrogen deficiency might down- or upregulate the MES set-point depending upon which bone surface is considered. To identify the role of acceleration in the adaptive response of rat bone to the vibratory stimulus, the loading frequency was kept constant while two accelerations were tested. The two accelerations applied were within the range 0.3–8 g, which has been shown to be effective and well tolerated in clinical studies [28, 29]. For this purpose, the response of the trabecular and cortical compartments to total-body vibration was evaluated in ovariectomized rats by peripheral quantitative computed tomographic (pQCT) analysis and histomorphometry.

Materials and Methods

Strain Gauge Implant and Recording

Three 3-month-old female Sprague-Dawley rats, weighing 250–275 g (Charles River Laboratories, Calco, Italy), were anesthetized and strain gauges (SA06008CL120; Vishay Micro-Measurements, Milan, Italy) were implanted according to the technique described by Rabkin et al. [30]. Briefly, a 1.5 cm incision was made over the anterior tibia. A single strain gauge was fixed on the tibial surface by histoacrylic glue. The lead wire of strain gauge A was passed subcutaneously along the back of the rat in order to exit at the back of the neck. The implant was waterproofed with polyurethane and RTV silicone rubber according to the supplier's instructions (Vishay Micro-Measurements). The gauge resistance was checked, and the lead wires exiting the neck were trimmed to expose a short length of wire (1 cm). Strains were measured by a bridge amplifier (P3, $\pm$0.1% accuracy and 1 microstrain resolution; Vishay Micro-Measurements) equipped with a static strain indicator and a digital data logger. Strain gauge recording was performed for 5 minutes and repeated three times in rats placed on the platform vibrating at 0.6 and 3 g peak-to-peak acceleration. The measurements were repeated on the

same animal 24 hours later and were consistent with the data of the previous day.

Vibration System and Data Acquisition

A National Instruments (Baltimore, MD) PCI-6036E Data Acquisition card was used to generate a sine wave to drive the vibration and to digitize an analog input signal from the sensor. Software was developed in LabView to control the amplitude and frequency of the sine wave output and to calculate the frequency and amplitude of the digitized input signal using a discrete Fourier transform operation. The frequency and amplitude data from the input signal were displayed on a chart as a function of time and logged to a text file for postprocessing (Science Wares, Falmouth, MA).

An accelerometer (A/120/VT; DJB Instruments, Verdun, France), attached to the vibrating plate, was used to generate the input signal controlling the amplitude. The input signal was amplified by a linear power amplifier (PA 100E; Gearing & Watson Electronics, East Sussex, UK) and transmitted to an E-M Actuator (PA 100E, Gearing & Watson Electronics) to generate the specific vibration over the neutral line (Fig. 1a). The actuator and the plate were inserted in a clear-walled cylinder on the floor. Vertical peak-to-peak displacement of the plate occurred without interference by the wall (0.5 mm clearance). Each rat was allowed to move freely on the plate, thus adding the vibratory stimulus to normal cage activity.

Vibration Protocol

Rats were housed in cages under controlled conditions (22 ± 2°C, 65% humidity, 12/12-hour light/darkness cycle). After receipt, rats were allowed to acclimatize for a week before ovariectomy or sham surgery. Ovariectomy was performed under anesthesia obtained with ketamine-xylazine, 0.075 mL/hg (Pfizer Italia, Milan, Italy), and xylazine, 0.025 mL/hg, i.p. (Rompum; Bayer, Milan, Italy). A total of 75 rats reached the end of the experiment, randomly divided into six groups: sham control (SHAM, $n = 14$); sham vibrated (SHAM-V) at 30 Hz, 0.6 g ($n = 11$) and at 30 Hz, 3g ($n = 10$); ovariectomized control (OVX, $n = 15$); ovariectomized vibrated (OVX-V) at 30 Hz, 0.6 g ($n = 11$) and at 30 Hz, 3g ($n = 14$). The number of animals varied from group to group because some died as a consequence of the anesthesia required for ovariectomy and/or pQCT analyses. Rats underwent whole-body vibration on the vibration platform for 20 minutes/day, 5 days/week, for 2 months. The net force acting on the rat tibia (during vibration applied between the knee joint and ankle joint) was estimated by assuming that the body weight is homogeneously distributed on the four

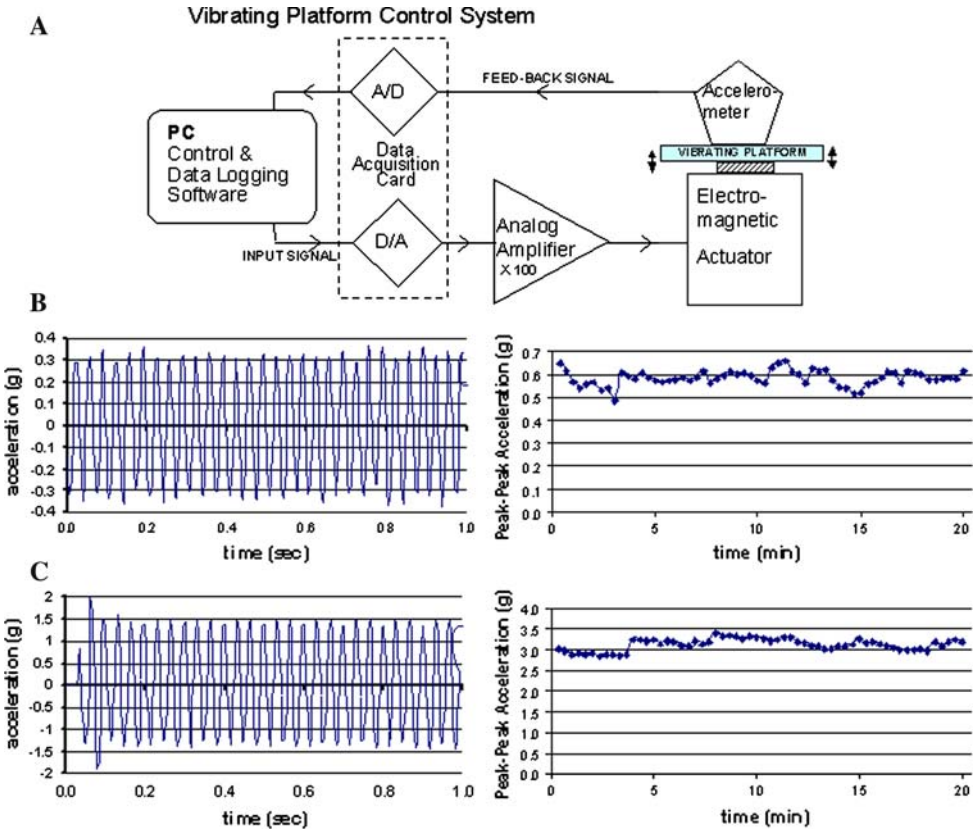

Fig. 1 Schematic representation of the vibrating platform control system (**A**). PC, personal computer; A/D, analogic/digital; D/A, digital/analogic. Typical readings of the input signal obtained by the accelerometer at 30 Hz and 0.6 g (**B**) and at 30 Hz and 3g (**C**). The signal remained steady over the experimental time

legs. Thus, in a 320 g rat, each tibia would bear a load of 80 g, or 0.78 N. Hence, the load increase by the acceleration superimposed over gravity yields a peak load of 1.25 N at 0.6 g and 3.14 N at 3 g on each tibia.

The control rats were placed on the vibration platform without vibration for the same amount of time as the vibrated rats. For the longitudinal study, pQCT analyses were performed at baseline, before starting the vibration procedure, and after 4 and after 8 weeks under light anesthesia. At the end of the experiment (8 weeks), all rats were killed by carbon dioxide inhalation and the tibiae excised and fixed in buffered formalin for further histomorphometric and pQCT analyses. The experimental protocol was approved by the local Institutional Animal Care and Use Committee (IACUC license 262, December 9, 2004, with subsequent addendum of May 10, 2005).

pQCT Measurements

pQCT measurements were performed using a Stratec Research SA+ pQCT scanner (Stratec Medizintechnik, Pforzheim, Germany) with a voxel size of 70 μm and a scan speed of 3 mm/second. In order to orient the long axes of the bones parallel to the image planes, the anesthetized animals (longitudinal study) and the excised bone specimens (cross-sectional study) were fixed with a plastic holder for the pQCT measurements. The correct longitudinal positioning was determined by means of an initial "scout scan." The bones were scanned in the horizontal plane using two consecutive cross-sectional images at 5 and 25 mm distal to the proximal end of the tibia. The scans were analyzed with pQCT software 6.00B using contour mode 2 and peel mode 2 with a threshold of 500 mg/cm^3 for the calculation of trabecular and total bone parameters at the metaphysis and with a threshold of 710 mg/cm^3 for cortical bone parameters at the diaphysis. The different thresholds of 500 and 710 mg/cm^3 for the metaphysis and diaphysis, respectively, were established to account for partial volume effect. The cortical bone density is lower at the metaphysis than at the diaphysis due to the thinner cortex. The threshold was therefore adjusted according to the cortical density to optimize accuracy.

The polar strength strain index (SSI) was calculated by the manufacturer's software as follows: $SSI = \Sigma_i = {}_{1,n}\, r_i^2 \bullet aCD/ND \bullet r_{max}$, where r is the distance of a voxel from the center of gravity, r_{max} is the maximum distance of a voxel from the center of gravity, a is the area of a voxel, CD is the cortical density, and ND is the density of normal cortical bone tissue, equal to 1,200 mg/cm^3, as measured by pQCT when no spaces are included. To account for changes in the mineralization of bone, and therefore for changes in material properties, the section modulus was normalized for this value in the pQCT software.

For the muscle analyses, peel mode 2 with a threshold of 40 mg/cm^3 was used to separate fat from muscle and contour mode 1 with a threshold of 280 mg/cm^3 was used to separate muscle from bone. According to the manufacturer, the estimated total effective radiation dose of the applied single measurement, including the "scout view" and two slices, was lower than 10 μSv/exam.

Histomorphometry

Rats were injected i.p. with oxytetracycline (40 mg/kg) on days 36 and 54 of the experimental period and killed at the end of the eighth week. The left tibia of rats from each group (SHAM, SHAM-V at 0.6 and 3g, OVX, OVX-V at at 0.6 and 3g) was dehydrated in a graded series of ethanol and embedded in polymethylmethacrylate. A single cross section (150 μm thick) was obtained using a SP 1600 diamond saw microtome (Leica, Milan, Italy) cutting system from three different regions: metaphyseal (5 mm distal to its condyles), mid-diaphyseal, and distal diaphyseal (distal to the fusion of the fibula on the tibia). Metaphyseal and mid-diaphyseal sections were microradiographed (MicroXray; Italstructure, Como, Italy) and analyzed by means of image analysis software (Lucia G; Laboratory Imaging, Prague, Czech Republic). The following parameters were measured: (1) in the metaphyseal region, bone volume/tissue volume (BV/TV), trabecular thickness (Tb.Th), trabecular number (Tb.N), and trabecular separation (Tb.S); (2) in the mid-diaphyseal region, total cross-sectional area (Tt.Ar), medullary area (Me.Ar), cortical bone area (CtB.Ar), total cross-sectional perimeter (Tt.Pm), medullary perimeter (Me.Pm), and cortical width (Ct.Wi). All sections were also examined under ultraviolet light by means of a Zeiss (Jena, Germany) Axiophot microscope using the previously mentioned image analysis software to evaluate tetracycline labeling at the bone cortex. Bone formation rate (BFR) was calculated by dividing the area of bone between the double labeling for the interlabel time at both the endosteal and periosteal sides. Mid-diaphyseal sections were also carefully polished, etched with a solution of HCl 0.1 N for 60 seconds, and gold palladium–coated for backscattered scanning electron microscopic (SEM) analysis. Nomenclature and abbreviations follow the recommendations of the American Society for Bone and Mineral Research.

Statistical Analysis

Statistical analysis was performed with the statistical package GraphPad Prism, version 4.00 for Windows (GraphPad Software, San Diego, CA, www.graphpad.com). Data were expressed as mean ± standard error of the mean. The significance of differences between

groups and between times in the longitudinal study was assessed by means of a two-way analysis of variance (ANOVA) for repeated measures and Bonferroni's multiple comparison test. The significance of differences between groups in the cross-sectional study was assessed by means of a one-way ANOVA and Bonferroni's multiple comparison test. SSI dependence on acceleration was assessed by means of a linear regression analysis. Histomorphometric data were compared by means of one-way ANOVA and the Student-Newmann-Keuls test.

Results

Vibration System and Strain Evaluation

The vibration system was tested under both vibration regimens (0.6 and 3 g) at each vibration cycle throughout the experimental time and found appropriate. Typical readings are shown in Figure 1b, c. In vivo strain data collected from the anteromedial surface of the tibia showed that the dynamic strain magnitudes induced at 30 Hz depended upon the peak-to-peak acceleration, i.e., 0.6 or 3 g. The mean peak-to-peak strain was 14.07 $\pm$ 5.09 $\mu\varepsilon$ at 0.6 g and 23.40 $\pm$ 7.53 $\mu\varepsilon$ at 3 g ($n = 3$). The loading frequency of the platform was transmitted to the strain gauge with no alteration as the dominant peak in the frequency domain coincided with the vibration frequency. However, the peak-to-peak strain increased by less than twofold (1.71-fold) in response to a fivefold increase in the loading amplitude.

pQCT Measurements

Longitudinal Evaluation in vivo

The in vivo pQCT measurements of cortical (Ct-BMD) and trabecular, volumetric bone mineral density (Tb-BMD) at the tibial metaphysis and diaphysis at baseline and at 4 and 8 weeks into the experiment for all groups are shown in Table 1. Ct-BMD of the tibial metaphysis and diaphysis increased slightly, but significantly, over time in all groups, whereas Tb-BMD significantly decreased in OVX groups and remained steady in the SHAM group. The vibration did not change Ct-BMD and was ineffective at preventing trabecular bone loss in OVX rats. No significant differences in Ct-BMD and Tb-BMD were observed between the vibrated and nonvibrated groups at all experimental times and at both vibration regimens applied. To further analyze the effect of vibration, the trabecular density distribution was evaluated. The results showed a shift of the density distribution in the OVX groups toward lower values, but the vibration did not significantly change the density distribution pattern in the presence or absence of estrogens (Fig. 2). pQCT analysis showed that ovariectomy also did not modify the muscle areas in all groups (data not shown).

Animal weights increased in all groups during the experiment; however, the weight of OVX animals increased more than that of SHAM animals, and the weight gain was not affected by the two vibration regimens (Fig. 3).

Cross-sectional Evaluation in vitro

In the SHAM group, vibration at both regimens did not induce any significant change in all the bone density and size parameters considered, both in the metaphysis (Table 2) and in the diaphysis (Table 3) of the tibia. In OVX animals, vibration at 3 g induced a significant increase of the total areas and of the cortical and medullary areas ($P < 0.01$) as well as the periosteal ($P < 0.01$) and the endosteal ($P < 0.05$) perimeters of the diaphysis (Table 3). Tb.BMD was significantly ($P < 0.001$) lower in the OVX groups than in the SHAM groups, but the difference was not significantly affected by vibration at both regimens (Table 2).

Polar SSI increased linearly in the OVX-V groups in proportion to the acceleration applied ($F = 11.342$, $P < 0.005$), reaching statistical significance ($P < 0.01$) at the 3 g vibration regimen (Fig. 4).

Histomorphometry

The static histomorphometric values measured in the tibial metaphysis are reported in Table 4. Except for Tb.Th, significant differences were observed between the SHAM and OVX groups, independent of the vibration regimen. No significant differences were found between the SHAM and SHAM-V groups or between the OVX and OVX-V groups at both vibration regimens (0.6 and 3 g). The static histomorphometric parameters measured in the mid-diaphyseal sections were not statistically different among groups; nonetheless, a tendency toward an increase of total cross-sectional and medullary areas in the OVX compared to the SHAM group was recognized (Table 4).

Examination of bone sections under ultraviolet light showed diffuse labeling at the metaphyseal level that did not allow optimal readings of the dynamic parameters. A measurable tetracycline double labeling was instead present at the mid-diaphyseal level in most sections, and the derived BFR was analyzed as a function of the vibration regimen and estrogen status. No significant differences were found between the vibration regimens in either the SHAM or OVX group. However, BFR at the bone surface was significantly ($P < 0.001$) greater in the OVX group (0.00897 $\pm$ 0.00399 mm^2/day) compared to the SHAM group (0.00492 $\pm$ 0.00291 mm^2/day).

Table 1 Longitudinal pQCT measurements of volumetric BMD in the tibiae

	SHAM			SHAM+0.6 g, 30 Hz			SHAM+3 g, 30 Hz		
	Basal	4 Weeks	8 Weeks	Basal	4 Weeks	8 Weeks	Basal	4 Weeks	8 Weeks
Diaphysis									
Ct-BMD	1,306.8 ± 15.1	1,350.6 ± 4.8**	1,369.1 ± 4.8**	1,326.4 ± 5.2	1,352.3 ± 3.0**	1,368.0 ± 3.1**	1,327.2 ± 5.8	1,355.6 ± 4.7*	1,366.5 ± 5.3**
Metaphysis									
Tb-BMD	382.9 ± 8.3	378.4 ± 9.7	385.1 ± 10.4	372.9 ± 8.6	378.3 ± 8.2	390.0 ± 8.9	365.2 ± 11.4	366.3 ± 13.3	368.0 ± 13.9
Ct-BMD	1,052.9 ± 9.0	1,116.0 ± 7.1**	1,134.3 ± 11.9**	1,045.9 ± 16.4	1,123.9 ± 10.9**	1,137.8 ± 9.5**	1,077.2 ± 9.9	1,121.7 ± 13.0*	1,154.8 ± 8.8**
	OVX			OVX+0.6 g, 30 Hz			OVX+3 g, 30 Hz		
	Basal	4 Weeks	8 Weeks	Basal	4 Weeks	8 Weeks	Basal	4 Weeks	8 Weeks
Diaphysis									
Ct-BMD	1,314.4 ± 9.5	1,355.6 ± 24.5*	1,367.4 ± 3.8**	1,325.5 ± 5.8	1,365.1 ± 5.3**	1,370.4 ± 6.5**	1,332.6 ± 5.0	1,354.6 ± 4.9*	1,366.8 ± 12.1*
Metaphysis									
Tb-BMD	368.8 ± 8.0	264.0 ± 11.8*	210.7 ± 4.0*	384.6 ± 13.3	280.4 ± 7.9**	229.2 ± 6.1**	360.2 ± 9.6	275.9 ± 11.8**	230.8 ± 13.8**
Ct-BMD	1,040.8 ± 11.9	1,099.9 ± 12.1**	1,133.2 ± 9.8**	1,046.6 ± 15.7	1,089.6 ± 15.8	1,129.7 ± 13.9**	1,070.5 ± 7.5	1,118.6 ± 13.5*	1,126.2 ± 15.9**

Ct-BMD, cortical bone mineral density; Tb-BMD, trabecular bone mineral density

* $P < 0.05$, ** $P < 0.01$ vs. basal ($n = 9$–13 rats/group)

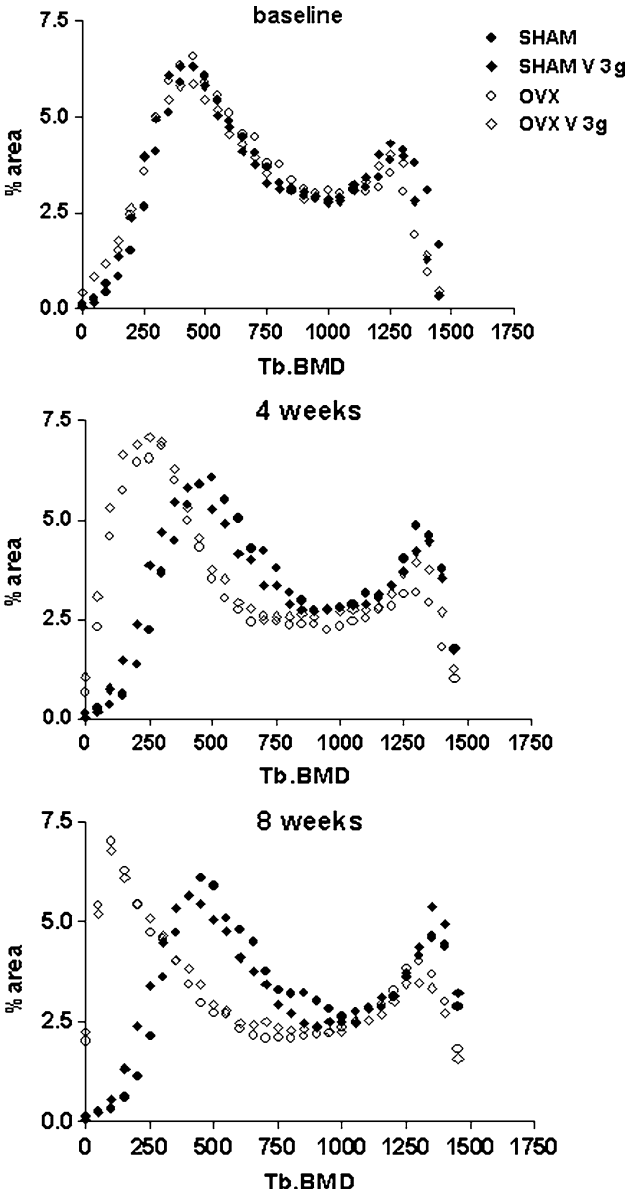

Fig. 2 Distribution of tibial Tb.BMD over the total bone area at baseline and after 4 and 8 weeks of daily vibration in the tibiae (metaphyses) of different groups

SEM analysis showed that in all animals the new bone laid down beyond labels is regular lamellar bone at both the endosteal (Fig. 5a) and periosteal (Fig. 5b) sides of the tibia.

Discussion

The current study has shown that low-amplitude, high-frequency whole-body vibration requires the absence of gonadal estrogens to be anabolic to bone at the specific vibration regimens applied. In OVX animals, vibration was effective on modeling of the bone cortex and its osteogenic

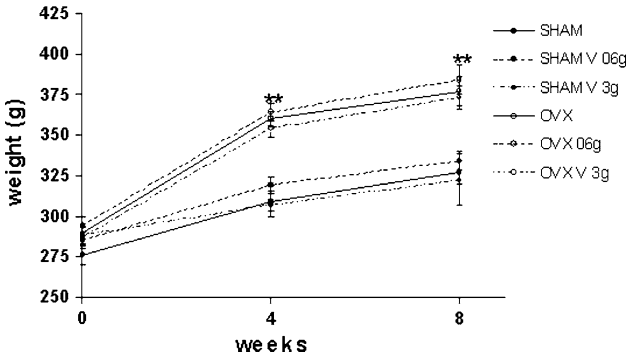

Fig. 3 Mean ± standard error of the mean of animal weights in the different groups at baseline and at 4 and 8 weeks. The two vibration regimens had no effect on weight. $^{**}P < 0.01$ OVX vs. SHAM

potential was dependent upon the amplitude of the vibratory stimuli applied. These results fit the view that trabecular and cortical compartments display a different sensitivity to a vibratory stimulus that may be modulated by the presence of estrogens. In fact, ovariectomy sensitizes periosteal bone apposition to the vibration. At the vibration amplitude of 3 g, enhanced periosteal apposition and endosteal resorption in the OVX rats resulted in an outward shift of bone mass from the neutral axis with a subsequent improvement of the SSI of the diaphyseal shaft. Since SSI defines bone resistance, it follows that the vibratory stimulus is able to work against the trabecular bone loss due to ovariectomy, enhancing the overall mechanical competence of the appendicular skeleton. This result was obtained by cross-sectional pQCT in vitro measurements, which are less affected by bone edge detection and positioning problems compared with in vivo longitudinal evaluation. These data confirmed previous findings obtained in OVX rats subjected to 25 Hz whole-body vibration in which vibration did not affect ovariectomy-induced endosteal resorption but preserved cortical strength by increasing periosteal formation [31]. The geometric changes observed between vibrated and nonvibrated OVX rats were also apparent by the histomorphometric analysis of the tibial diaphysis, although the results did not reach statistical significance. Besides quantitative evaluation, the histological analysis gave further insights into understanding the effect of vibration on bone. SEM analysis of the bone sections showed that the new superficial bone laid down between the two labels was regular lamellar bone, thus suggesting that the periosteal effect of vibration in OVX rats fits with the physiological bone remodeling pattern. In fact, any nonspecific stimulus upon the periosteum is generally associated to the deposition of an irregular pattern of lamellae. Furthermore, the histomorphometric observation that BFR is significantly activated in OVX rats indicates that OVX expands the bone cellular pool that is the target of the mechanical signal,

Table 2 Cross-sectional evaluation of structural geometric properties at tibial diaphysis evaluated ex vivo after 8 weeks (treatment)

Parameters	SHAM	SHAM+0.6 g, 30 Hz	SHAM+3 g, 30 Hz	OVX	OVX+0.6 g, 30 Hz	OVX+3 g, 30 Hz
Ct-BMD (mg/cm^3)	1,380.7 ± 5.8	1,372.6 ± 2.9	1,387.3 ± 2.6	1,380.2 ± 3.6	1,379.2 ± 6.2	1,392.2 ± 4.4
Tt.Ar (mm^2)	5.90 ± 0.10	5.67 ± 0.13	5.92 ± 0.15	6.00 ± 0.11	6.28 ± 0.16	6.58 ± 0.09**
Md.Cn.Ar (mm^2)	0.71 ± 0.03	0.70 ± 0.05	0.67 ± 0.06	0.73 ± 0.04	0.80 ± 0.04	0.88 ± 0.06
Ct.Ar (mm^2)	4.81 ± 0.10	4.74 ± 0.11	4.83 ± 0.13	4.86 ± 0.09	5.05 ± 0.11	5.27 ± 0.07**
Ct.Th (mm)	0.78 ± 0.01	0.77 ± 0.02	0.79 ± 0.02	0.78 ± 0.01	0.79 ± 0.01	0.80 ± 0.01
Ps.Pm (mm)	8.61 ± 0.07	8.58 ± 0.09	8.62 ± 0.10	8.68 ± 0.08	8.88 ± 0.11	9.09 ± 0.06**
Es.Pm (mm)	3.70 ± 0.05	3.74 ± 0.11	3.68 ± 0.10	3.78 ± 0.07	3.91 ± 0.12	4.06 ± 0.08*

Ct-BMD, cortical bone mineral density; Tt.Ar, total area; Md.Cn.Ar, medullary canal area; Ct.Ar, cortical area; Ct.Th, cortical thickness; Ps.Pm, periosteal perimeter; Es.Pm, endosteal perimeter

* $P < 0.05$, ** $P < 0.01$ vs. OVX (n = 9–13 rats/group)

Table 3 Cross-sectional evaluation of structural geometric properties at the metaphysis of tibiae, evaluated ex vivo after 8 weeks

Parameters	SHAM	SHAM+0.6 g, 30 Hz	SHAM+3g, 30 Hz	OVX	OVX+0.6 g, 30 Hz	OVX+3 g, 30 Hz
Ct-BMD (mg/cm^3)	1,142.4 ± 14.4	1,149.4 ± 9.2	1,147.0 ± 15.3	1,136.1 ± 12.0	1,159.6 ± 12.1	1,149.5 ± 10.4
Tb-BMD (mg/cm^3)	396.2 ± 9.3	395.6 ± 9.1	377.9 ± 9.7	251.1 ± 16.08**	250.3 ± 9.7**	252.6 ± 9.8**
Tt.Ar (mm^2)	16.54 ± 0.92	15.69 ± 0.50	17.17 ± 0.68	18.29 ± 0.54	17.18 ± 0.87	18.23 ± 0.64
Tb.Ar (mm^2)	3.15 ± 0.63	3.36 ± 0.55	4.00 ± 0.70	8.48 ± 0.48**	7.98 ± 0.62**	8.81 ± 0.43**
Ct.Ar (mm^2)	8.49 ± 0.67	8.23 ± 0.40	8.57 ± 0.58	7.12 ± 0.16	7.10 ± 0.23	7.00 ± 0.20
Ct.Th (mm)	0.70 ± 0.05	0.69 ± 0.04	0.69 ± 0.04	0.53 ± 0.02**	0.54 ± 0.01*	0.52 ± 0.01**
Ps.Pm (mm)	14.36 ± 0.41	14.19 ± 0.25	14.67 ± 0.29	15.14 ± 0.22	14.78 ± 0.37	15.11 ± 0.27
Es.Pm (mm)	9.98 ± 0.40	9.89 ± 0.32	10.36 ± 0.32	11.79 ± 0.54	11.37 ± 0.39	11.84 ± 0.28

Ct-BMD, cortical bone mineral density; Tb-BMD, trabecular bone mineral density; Tt.Ar, total area; Tb.Ar, trabecular area; Ct.Ar, cortical area; Ct.Th, cortical thickness; Ps.Pm, periosteal perimeter; Es.Pm, endosteal perimeter

* $P < 0.01$, ** $P < 0.001$ vs. SHAM (n = 9–13 rats/group)

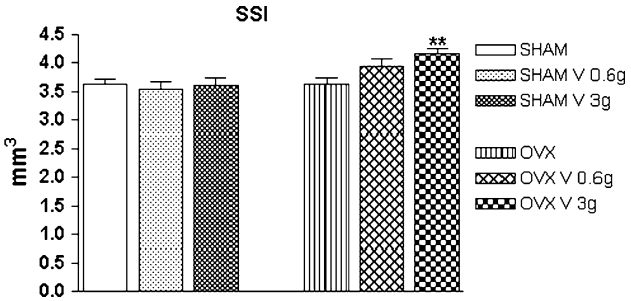

Fig. 4 Mean ± standard error of the mean of SSI obtained by pQCT analysis of excised tibiae at the end of the experimental time (8 weeks) in the different groups. **$P < 0.01$ vs. SHAM and OVX

suggesting that bone should be in an activated state to respond to mechanical stimuli.

This study failed to observe any cortical bone response to the vibratory stimulus in the intact animals, in agreement with the observations of others that (1) low-amplitude (0.1–0.3 N) vibration at broad frequencies (0–50 Hz) did not cause formation of additional cortical bone when applied to the female mouse ulna in uniaxial compression [32]; (2) loading the female mouse ulna with a 0.3 N vibration signal alone, not superimposed upon an osteogenic stimulus, did not result in any new cortical bone formation [9]; (3) adult female sheep exposed to low-level (0.3 g), high-frequency (30 Hz) mechanical signals did not show any change in the bone cortex as assessed by pQCT and histomorphometry [5].

The demonstration that vibration loses its osteogenic potential when the estrogen axis is intact is in agreement with the recent observations that low-dose 17α-ethynylestradiol suppresses the periosteal response to axial loading of the ulna of male rats [33] and that ERβ knockout mice show improved bone formation [26] and increased periosteal responsiveness [34] after mechanical loading. Such observations support the view that estrogens act as negative modulators of the mechanotransduction process at the periosteal surface via ERβ signaling. It is therefore conceivable that estrogens might down- or upregulate the MES set-point depending upon which signaling pathway is activated. In a state of estrogen deficiency, as in menopause, the lack of inhibitory ERβ signaling might activate a compensatory mechanism in order to maintain bone mechanical resistance despite the loss of bone at the endocortical surface. The outward displacement of the thinning cortex could be a target for mechanical

Table 4 Static histomorphometric evaluation of the tibiae

	SHAM	SHAM+0.6 g, 30 Hz	SHAM+3 g, 30 Hz	OVX	OVX+0.6 g, 30 Hz	OVX+3 g, 30 Hz
Metaphysis						
BV/TV (%)	47.43 ± 7.90	48.38 ± 3.78	46.46 ± 13.34	21.73 ± 6.00**	25.07 ± 6.53*	18.16 ± 5.23*
Tb.Th (μm)	56.69 ± 13.16	60.40 ± 20.11	63.08 ± 15.74	47.07 ± 12.53	60.19 ± 6.26	50.50 ± 14.12
TB.N (/mm^2)	6.50 ± 1.47	6.28 ± 1.02	6.01 ± 1.16	3.20 ± 0.94**	3.16 ± 0.59*	2.56 ± 0.96*
Tb.S (μm)	104.46 ± 41.39	102.01 ± 14.04	109.15 ± 45.99	338.45 ± 195.47**	267.25 ± 74.83	411.48 ± 235.02
Diaphysis						
Tt.Ar (mm^2)	6.00 ± 0.44	5.80 ± 0.54	6.01 ± 0.24	6.12 ± 0.53	6.27 ± 0.64	6.35 ± 0.50
Me.Ar (mm^2)	1.44 ± 0.36	1.40 ± 0.25	1.52 ± 0.19	1.50 ± 0.27	1.60 ± 0.46	1.69 ± 0.25
CtB.Ar (mm^2)	4.55 ± 0.23	4.40 ± 0.33	4.49 ± 0.30	4.61 ± 0.33	4.66 ± 0.33	4.65 ± 0.31
Tt.Pm (mm)	9.50 ± 0.43	9.17 ± 0.35	9.55 ± 0.34	9.67 ± 0.44	9.74 ± 0.63	9.67 ± 0.37
Me.Pm (mm)	4.46 ± 0.67	4.47 ± 0.32	4.74 ± 0.25	4.73 ± 0.47	4.86 ± 0.76	4.88 ± 0.37
Ct.Wi (μm)	646 ± 48	642 ± 36	622 ± 58	633 ± 31	639 ± 67	635 ± 37

BV/TV, bone volume/total volume; Tb.Th, trabecular thickness; Tb.N, trabecular number; Tb.S, trabecular separation; Tt.Ar, total cross-sectional area; Me.Ar, medullary area; CtB.Ar, cortical bone area; Tt.Pm, total cross-sectional perimeter; Me.Pm, medullary perimeter; Ct.Wi, cortical width

Mean value ± standard deviation; each value is derived from a single serial cross section taken from the left tibia

* $P < 0.01$ vs. basal

** $P < 0.001$ vs. SHAM ($n = 5$–8 rats/group)

intervention therapy in postmenopausal osteoporosis as well as for drug development [35].

No trabecular effect was observed at the vibration regimens applied, in contrast to the original thought that low-amplitude, high-frequency strain rates are anabolic to cancellous, but not to cortical, bone [5]. Besides potential species-specific differences in the sensitivity to mechanical stimuli, it might be possible that different postures on the vibration platform among the different animal models will determine different effects of vibration upon the strain rate at the trabecular compartment. Unlike sheep, rats as well as mice move freely during a cycle of whole-body vibration and they are, therefore, subjected to a vibratory stimulus that can change according to body posture. Such changes can be potentially dampened by the viscoelastic nature of the muscle–tendon apparatus [32]. The lack of a linear relationship between the increase in the strain and the increase in the acceleration is in agreement with this view.

Since the vibratory stimulus was ineffective at altering trabecular bone density and preventing postovariectomy trabecular bone loss, it might be that it has not reached the threshold sensitivity of the trabecular compartment. It is conceivable that the vibratory stimulus perceived by the trabecular compartment might require higher frequencies to reach the osteogenic threshold and subsequently activate a transduction pathway of the mechanical stimuli not necessarily related to matrix strain [36]. It has been reported that both cortical and trabecular BFRs were significantly increased in vibrated animals compared to controls when vibration was applied at 90 Hz, while at 45 Hz there was no significant increase in either cortical or trabecular BFR [37]. As pointed out by Judex et al. [37], it is possible that the adaptive response to low-amplitude, high-frequency mechanical regimens does not follow the rules of strain in the low-frequency domain. It follows that effects upon bone induced by whole-body vibration and the sensitivity of the bone compartment to a specific vibration regimen might be due to the activation of different mechanisms of signal transduction, not necessarily working in a linear magnitude–dependent manner [38, 39]. How differences in frequency and/or amplitude alter the efficacy of low-amplitude, high-frequency mechanical stimuli is largely unknown. How the specific mechanical parameters modulate the different bone compartment sensitivities is likewise unknown.

The increase in Ct-BMD in the SHAM group during the experimental time indicates that the animals had not yet reached peak bone mass, in agreement with the observations of others [40, 41]. This is an important limitation of the study as it was not possible to discriminate the influence of skeletal growth on the whole-body vibration effect. Nevertheless, it should be considered that (1) pQCT does not distinguish between material and structural properties of bone (it follows that as long as the secondary mineralization process takes place, increasing volumetric density [material property] does not imply a parallel increment in bone mass [structural property]) and (2) cross-sectional bone area of rats and humans continues to increase slowly throughout life [42]. Therefore, even older rats would undergo radial growth and the interpretation of the results

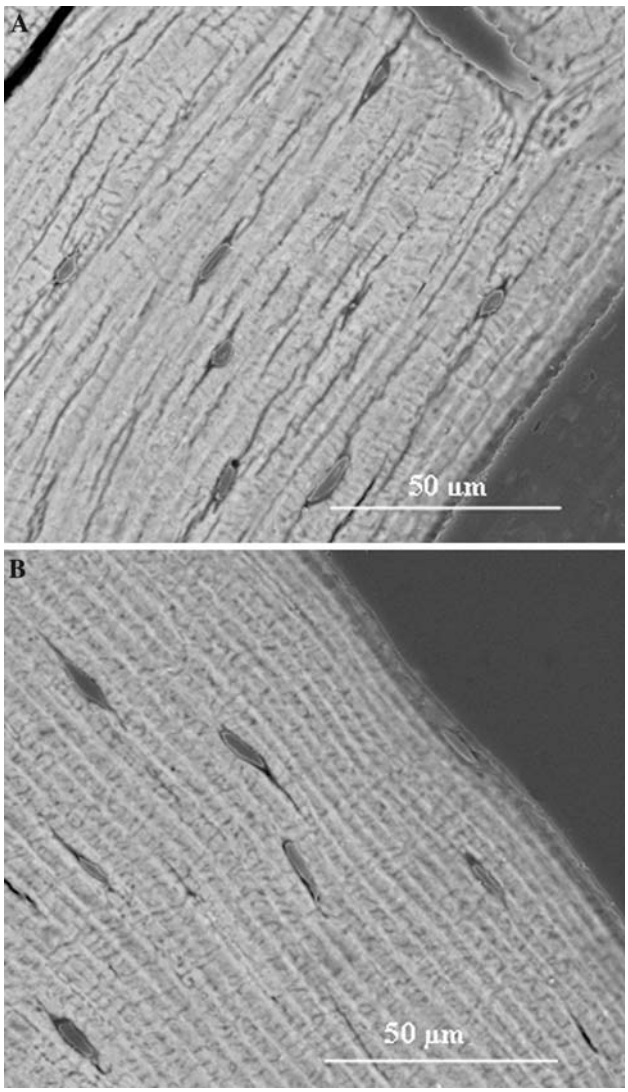

Fig. 5 SEM micrograph of an endosteal portion (**A**) of the tibial mid-diaphysis and of a periosteal portion (**B**) of the tibial mid-diaphysis where new lamellar bone is present (magnifiction x2,000, bar = 50 µm). This was observed in the rats of all groups

would be equally limited, the whole-body vibration effect being potentially dependent on growth or bone homeostasis processes.

This study suggests that noninvasive mechanical loading, far below that associated with exercise or increased fracture risk, could represent a unique means of enhancing bone mechanical competence, particularly in the estrogen-depleted elderly. Well-designed studies in elderly individuals with osteoporosis are lacking, and the adaptive responses to vibration are not yet completely understood. Safety and efficacy studies of this type of loading in humans are required. When the body is subjected to chronic whole-body vibrations, spinal degeneration is likely to be one of the deleterious outcomes [43]. However, as discussed by Christiansen and Silva [38], such studies have almost always examined the effect of vibration on seated subjects, and resonance peaks have typically been found at frequencies below 10 Hz. Since vibration loading as a potential treatment for osteoporosis would be applied to standing subjects at much higher frequencies, it can be assumed that the risk of low back pain is reduced. Moreover, the exposure of humans to 3 g for 1 minute would be equivalent to about 30 m/second^2, thus within the limits established by European Union guidelines [44]. Nevertheless, it should be taken into account that the actual accelerations in the human body are much smaller than those measured on the plate due to the dampening effect of soft tissue structures, as discussed above. When 8-month vertical whole-body vibration was applied in a controlled randomized trial, it was well tolerated up to 8 g [29].

In conclusion, this study strengthens the view that whole-body vibration has osteogenic potential in a rat animal model. Since the vibratory stimulus appears to require the lack of gonadal estrogens to be effective on the outward displacement of the cortex, it might be effective as a nonpharmacological adjuvant in the treatment of postmenopausal osteoporosis by potentially increasing bone size and reducing the risk of fracture.

The authors thank Erik Karplus (Science Wares, Falmouth, MA), who designed the software for the control and data acquisition of the vibration system. This study was supported by the Italian Ministry of Research (COFIN 2004–2006).

References

1. Rubin CT, Mcleod KJ, Bain SD (1990) Functional strains and cortical bone adaptation: epigenetic assurance of skeletal integrity. J Biomech 23(Suppl 1):43–54
2. Rubin CT, Sommerfield DW, Judex S, Qin Y (2001) Inhibition of osteopenia by low magnitude, high frequency mechanical stimuli. Drug Discov Today 6:848–858
3. Rubin CT, Turner AS, Bain S, Mallinckrodt C, McLeod K (2001) Anabolism. Low mechanical signals strengthen long bones. Nature 412:603–604
4. Jankovich JP (1972) The effects of mechanical vibration on bone development in the rat. J Biomech 5:241–250
5. Rubin C, Turner AS, Mallinckrodt C, Jerome C, Mcleod K, Bain S (2002) Mechanical strain, induced noninvasively in the high-frequency domain, is anabolic to cancellous bone, but not cortical bone. Bone 30:445–52
6. Judex S, Zhong N, Squire ME, Ye K, Donahue LR, Hadjiargyrou M, Rubin CT (2005) Mechanical modulation of molecular signals which regulate anabolic and catabolic activity in bone tissue. J Cell Biochem 94:982–994
7. Tanaka SM, Li J, Duncan RL, Yokota H, Burr DB, Turner CH (2003) Effects of broad frequency vibration on cultured osteoblasts. J Biomech 36:73–80
8. Usui Y, Zerwekh JE, Vanharanta H, Ashman RB, Mooney V (1989) Different effects of mechanical vibration on bone ingrowth into porous hydroxyapatite and fracture healing in a rabbit model. J Orthop Res 7:559–567

9. Tanaka SM, Alam I, Turner CH (2003) Stochastic resonance in osteogenic response to mechanical loading. FASEB J 17:313–314
10. Oxlund BS, Ortoft G, Andreassen TT, Oxlund H (2003) Low-intensity, high-frequency vibration appears to prevent the decrease in strength of the femur and tibia associated with ovariectomy of adult rats. Bone 32:69–77
11. Flieger J, Karachalios TH, Khaldi L, Raptou P, Lyritis G (1998) Mechanical stimulation in the form of vibration prevents postmenopausal bone loss in ovariectomized rats. Calcif Tissue Int 63:510–514
12. Frost HM (1987) Bone mass and the mechanostat: a proposal. Anat Rec 219:1–9
13. Frost HM (1983) A determinant of bone architecture. The minimum effective strain. Clin Orthop 175:286–292
14. Frost HM (1987) The mechanostat: a proposed pathogenic mechanism of osteoporoses and the bone mass effects of mechanical and non mechanical agents. Bone Miner 2:73–85
15. Lanyon LE, Sherry TM (2001) Perspective. Postmenopausal osteoporosis as a failure of bone's adaptation to functional loading: a hypothesis. J Bone Miner Res 16:1937–1947
16. Lanyon LE, Armstrong V, Ong D, Zaman G, Price J (2004) Is estrogen receptor α key to controlling bones' resistence to fracture? J Endocrinol 182:183–191
17. Jessop HL, Sjoberg M, Cheng MZ, Zaman G, Weeler-Jones CP, Lanyon LE (2001) Mechanical strain and estrogen activate estrogen receptor alpha in bone cells. J Bone Miner Res 16:1045–1055
18. Ehrlich PJ, Noble BS, Jessop HL, Stevens HY, Mosley JR, Lanyon LE (2002) The effect of in vivo mechanical loading on estrogen receptor alpha expression in rat ulnar osteocytes. J Bone Miner Res 17:1646–1655
19. Lee K, Jessop HL, Suswillo R, Zaman G, Lanyon L (2003) Endocrinology: bone adaptation requires oestrogen receptor-alpha. Nature 424:389
20. Zaman G, Jessop HL, Muzylak M, De Souza RL, Pitsillides AA, Price JS, Lanyon LL (2006) Osteocytes use estrogen receptor α to respond to strain but their ERα content is regulated by estrogen. J Bone Miner Res 21:1297–1306
21. Bass SL, Saxon LK, Daly RM, Turner CH, Robling AG, Seeman E, Stuckey S (2002) The effect of mechanical loading on the size and shape of bone in pre-, peri-, and postpubertal girls: a study in tennis players. J Bone Miner Res 17:2274–2280
22. Ahlborg HG, Johnell O, Turner CH, Rannevik G, Karlsson MK (2003) Bone loss and bone size after menopause. N Engl J Med 349:327–334
23. Vanderschueren D, Venken K, Ophoff J, Bouillon R, Boonen S (2006) Sex steroids and the periosteum: reconsidering the roles of androgens and estrogens in periosteal expansion. J Clin Endocrinol Metab 91:378–382
24. Duan Y, Beck TJ, Wang XF, Seeman E (2003) Structural and biomechanical basis of sexual dimorphism in femoral neck fragility has its origins in growth and aging. J Bone Miner Res 18:1766–1774
25. Bouillon R, Bex M, Vanderschueren D, Boonen S (2004) Estrogens are essential for male pubertal periosteal bone expansion. J Clin Endocrinol Metab 89:6025–6029
26. Saxon LK, Turner CH (2005) Estrogen receptor β: the antimechanostat? Bone 36:185–192
27. Westerlind KC, Wronski TJ, Ritman EL, Luo ZP, An KN, Bell NH, Turner RT (1997) Estrogen regulates the rate of bone turnover but bone balance in ovariectomized rats is modulated by prevailing mechanical strain. Proc Natl Acad Sci USA 94:4199–4204
28. Gilsanz V, Wren TA, Sanchez M, Dorey F, Judex S, Rubin C (2006) Low-level, high-frequency mechanical signals enhance musculoskeletal development of young women with low BMD. J Bone Miner Res 21:1464–1474
29. Torvinen S, Kannus P, Sievanen H, Jarvinen TA, Pasanen M, Kontulainen S, Nenonen A, Jarvinen TL, Paakkala T, Jarvinen M, Vuori I (2003) Effect of 8-month vertical whole-body vibration on bone, muscle performance, and body balance: a randomized controlled study. J Bone Miner Res 18: 876–884
30. Rabkin BA, Szivek JA, Schonfeld JE, Halloran BP (2001) Long term measurement of bone strain in vivo: the rat tibia. J Biomed Mater Res B Appl Biomater 58:277–281
31. Ioannidis GV, Skarantavos G, Raptou P, Khaldi L, Karachalios TH, Lyritis GP (2000) Whole-body vibrations induce periosteal bone formation in ovariectomised rats. J Musculoskelet Neuronal Interact 1:70–71
32. Castillo AB, Alam I, Tanaka SM, Levenda J, Li J, Warden SJ, Turner CH (2006) Low-amplitude, broad-frequency vibration effects on cortical bone in mice. Bone 39:1087–1096
33. Saxon LK, Turner CH (2006) Low-dose estrogen treatment suppresses periosteal bone formation in response to mechanical loading. Bone 39:1261–1267
34. Saxon LK, Robling AG, Castillo AB, Mohan S, Turner CH (2007) The skeletal responsiveness to mechanical loading is enhanced in mice with a null mutation in estrogen receptor-beta. Am J Physiol Endocrinol Metab 293:E484–E491
35. Seeman E (2007) The periosteum—a surface for all seasons. Osteoporos Int 18:123–128
36. Garman R, Gaudette G, Donahue LR, Rubin C, Judex S (2007) Low-level accelerations applied in the absence of weight bearing can enhance trabecular bone formation. J Orthop Res 25:732–740
37. Judex S, Lei X, Han D, Rubin C (2007) Low-magnitude mechanical signals that stimulate bone formation in the ovariectomized rat are dependent on the applied frequency but not on the strain magnitude. J Biomech 40:1333–1339
38. Christiansen BA, Silva MJ (2006) The effect of varying magnitudes of whole-body vibration on several skeletal sites in mice. Ann Biomed Eng 34:1149–1156
39. Warden SJ, Turner CH (2004) Mechanotransduction in the cortical bone is most efficient at loading frequencies of 5–10 Hz. Bone 34:261–270
40. Beamer WG, Donahue LR, Rosen CJ, Baylink DJ (1996) Genetic variability in adult bone density among inbred strains of mice. Bone 18:397–403
41. Iida H, Fukuda S (2002) Age-related changes in bone mineral density, cross-sectional area and strength at different skeletal sites in male rats. J Vet Med Sci 64:29–34
42. Allen MR, Hock JM, Burr DB (2004) Periosteum: biology, regulation, and response to osteoporosis therapies. Bone 35:1003–1012
43. Cardinale M, Rittweger J (2006) Vibration exercise makes your muscles and bones stronger: fact or fiction? J Br Menopause Soc 12:12–18
44. Griffin MJ (2004) Minimum health and safety requirements for workers exposed to hand-transmitted vibration and whole-body vibration in the European Union: a review. Occup Environ Med 61:387–397